

# APPLIED COMPUTING, MATHEMATICS AND STATISTICS GROUP

Division of Applied Management and Computing

## Fracture toughness of wood based on experimental near-tip displacement fields and orthotropic theory

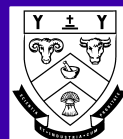
Sandhya Samarasinghe and Don Kulasiri

Research Report No:99/02  
January 1999

ISSN 1174-6696

# RESEARCH REPORT

LINCOLN  
UNIVERSITY  
*Te Whare Wānaka O Aoraki*



## **Applied Computing, Mathematics and Statistics**

The Applied Computing, Mathematics and Statistics Group (ACMS) comprises staff of the Applied Management and Computing Division at Lincoln University whose research and teaching interests are in computing and quantitative disciplines. Previously this group was the academic section of the Centre for Computing and Biometrics at Lincoln University.

The group teaches subjects leading to a Bachelor of Applied Computing degree and a computing major in the Bachelor of Commerce and Management. In addition, it contributes computing, statistics and mathematics subjects to a wide range of other Lincoln University degrees. In particular students can take a computing and mathematics major in the BSc.

The ACMS group is strongly involved in postgraduate teaching leading to honours, masters and PhD degrees. Research interests are in modelling and simulation, applied statistics, end user computing, computer assisted learning, aspects of computer networking, geometric modelling and visualisation.

### **Research Reports**

Every paper appearing in this series has undergone editorial review within the ACMS group. The editorial panel is selected by an editor who is appointed by the Chair of the Applied Management and Computing Division Research Committee.

The views expressed in this paper are not necessarily the same as those held by members of the editorial panel. The accuracy of the information presented in this paper is the sole responsibility of the authors.

This series is a continuation of the series "Centre for Computing and Biometrics Research Report" ISSN 1173-8405.

### **Copyright**

Copyright remains with the authors. Unless otherwise stated permission to copy for research or teaching purposes is granted on the condition that the authors and the series are given due acknowledgement. Reproduction in any form for purposes other than research or teaching is forbidden unless prior written permission has been obtained from the authors.

### **Correspondence**

This paper represents work to date and may not necessarily form the basis for the authors' final conclusions relating to this topic. It is likely, however, that the paper will appear in some form in a journal or in conference proceedings in the near future. The authors would be pleased to receive correspondence in connection with any of the issues raised in this paper. Please contact the authors either by email or by writing to the address below.

Any correspondence concerning the series should be sent to:

The Editor  
Applied Computing, Mathematics and Statistics Group  
Applied Management and Computing Division  
PO Box 84  
Lincoln University  
Canterbury  
NEW ZEALAND

Email: [computing@lincoln.ac.nz](mailto:computing@lincoln.ac.nz)

# FRACTURE TOUGHNESS OF WOOD BASED ON EXPERIMENTAL NEAR -TIP DISPLACEMENT FIELDS AND ORTHOTROPIC THEORY

Sandhya Samarasinghe, MSc(Eng), MS, PhD  
*Natural Resources Engineering Group, Lincoln University, NZ*

Don Kulasiri, BSc(Eng), MS, PhD  
*Applied Computing, Mathematics and Statistics Group, Lincoln University, NZ*

## SUMMARY

Fracture toughness of New Zealand pinus radiata in TL opening mode was determined from the displacement fields obtained from digital image correlation for about 400 data points within a  $7 \times 9 \text{ mm}^2$  area in front of the tip in conjunction with orthotropic fracture theory. Representative material properties obtained experimentally were used in the theoretical formulae. There was a significant correlation between theory and experiments. Stress intensity factor thus obtained increases nonlinearly with applied load and was consistently higher than that obtained from standard formula revealing a much larger correction factor than that given in handbooks. Fracture toughness obtained from the developed relationship showed a tendency to vary under the combined influence of density and crack angle to RL plane in a nonlinear manner. A relationship was also found to express the combined influence of density and grain angle on the Young's modulus ( $E_L$ ), measured from bending specimens corresponding to fracture specimens. The latter relationship can be used to simulate  $E_L$  and obtain a simplified expression for fracture toughness in terms of density and crack angle to RL plane.

## 1. INTRODUCTION

Structural wood members contain natural or artificial defects such as knots, drying checks, splits, and machined notches and holes that become stress raisers within the material. The nature and influence of such stress raisers on the stresses and strains in their vicinity has been the focus of fracture mechanics. In the study of fracture, three fracture modes are generally specified: opening mode, shear-mode, and twisting-mode. In opening mode fracture forces are applied perpendicular to crack, in shear-mode forces are applied in the crack plane parallel to crack, and in twisting-mode they are applied in the crack plane but perpendicular to the crack. Each of these modes is associated with a stress intensity factor,  $K_I$ ,  $K_{II}$ ,  $K_{III}$ , respectively which indicates the level of stress increase in the vicinity of a crack. For an orthotropic material like timber, there are six fracture systems for the three orthotropic planes but in many practical situations, fracture is relevant in TL and RL planes only and many a time fracture occurs in mixed-mode. (Here, first letter denotes direction normal to crack plane and second one denotes direction of crack.) Examples are horizontal and vertical cracks in beams and cracks emanating from holes of loaded bolted connections. In this paper, a detailed study of mode-I fracture in TL system is reported.

Fracture toughness allows to determine critical crack geometry for a particular situation. Therefore, knowledge of fracture toughness in RL and TL modes, which are the weakest, is essential in the design of most structural members. There are two basic theoretical approaches to formulate stress intensity factors. The earliest approach is based on energy to fracture as derived by Griffith [1]. He postulated that fracture occurs when strain energy density exceeds the work required to form new surfaces. This was applicable to brittle glass he tested but didn't apply to engineering materials like steel and aluminum. Irwin [2,3] proposed that there must be other energy absorbing mechanisms near the tip and introduced the concept of small scale yielding near the tip thereby laying the foundation for linear elastic fracture mechanics. The parameter derived in this approach is the strain energy release rate ( $G$ ), which Irwin [2] showed equal to  $K^2/E$  where  $K$  is stress intensity factor and  $E$  is Young's modulus.

The other approach involves the use of governing differential equations for a body without cracks and the modification of them to accommodate stress free crack boundaries. Using this approach a major theoretical effort has gone into characterizing the crack tip stress and displacement fields and stress intensity factors for linear elastic isotropic materials [4, 5]. Wood being an orthotropic material, near tip fields for an orthotropic material are relevant. Sih et. al. [6]

extended the Westergaard's [4] approach to formulate stress and displacement fields near a tip of a remotely loaded orthotropic plate in tension and shear. This derivation assumes that the material is homogeneous, truly orthotropic and material properties in a given direction are constant. The crack opening mode displacement for an orthotropic plate remotely loaded in tension as given by Sih et al.[6] is shown in Eq.(1)

$$v = K_I \sqrt{\frac{r}{2\pi}} \operatorname{Re} \left[ \frac{1}{\mu_1 - \mu_2} (\mu_1 q_2 \sqrt{\cos\theta + \mu_2 \sin\theta} - \mu_2 q_1 \sqrt{\cos\theta + \mu_1 \sin\theta}) \right] \quad (1)$$

where  $v$  is vertical displacement in the direction perpendicular to crack,  $K_I$  is mode-I stress intensity factor,  $\operatorname{Re}$  is real value of the expression within square brackets,  $\mu_1$ ,  $\mu_2$ ,  $q_1$ ,  $q_2$  are functions of material properties as shown below.

The values of  $\mu$  are complex roots of the characteristic equation corresponding to the governing differential equation for two-dimensional anisotropic elasticity as shown in Eq.(2) below.

$$b_{11}\mu^4 + (2b_{12} + b_{66})\mu^2 + b_{22} = 0 \quad (2)$$

where for TL plane of loading for wood,

$$b_{11} = \frac{1}{E_L} - \frac{\nu_{RL}^2}{E_R}; \quad b_{22} = \frac{1}{E_T} - \frac{\nu_{RT}^2}{E_R};$$

$$b_{12} = -\left[ \frac{\nu_{TL}}{E_T} + \frac{\nu_{RL}\nu_{RT}}{E_R} \right]; \quad b_{66} = \frac{1}{G_{LT}}.$$

The parameters  $E$ ,  $\nu$ , and  $G$  with subscripts denote Young's modulus in L, R, T directions, poisson ratio in TL, RL, and RT modes, and shear modulus in LT plane, respectively.

With respect to wood several issues need to be addressed in the use of theoretical formulae. Triboulot et al. [7] showed that for constant average orthotropic wood properties, near tip stresses obtained from the finite element method and analytical formulae are similar. This can be expected because, in the linear elastic fracture theory for orthotropic materials, it is assumed

that the material properties in a given direction are constant and therefore, fracture toughness for a particular mode is constant. However, it is well known from wood literature that the fracture toughness varies significantly with density which varies from early wood to latewood, along the height of the stem and along a radius of the cross section [8]. Moreover, wood is not truly orthotropic unless the member is cut farther away from the center of a large diameter stem.

In wood growth rings are approximately cylindrical or conical and therefore, for a particular piece cut from a flat-sawn board, Young's modulus at a point not only varies with density but also grain angle. Our study showed that the maximum load carried by fracture specimens increases with crack angle to the RL plane. Mall et al. [9] have also stated that the fracture toughness in TL mode depends on the angle of the crack to the RL plane along which the crack always propagates in this mode. If a crack lies in the RL plane, fracture toughness is smaller than that for a crack inclined to the RL plane. The above considerations must be addressed if the theory were to be used for making realistic predictions and this paper attempts to address these issues.

Another issue is the geometry correction factor. It has been shown from theory that  $K$  can be related to remotely applied stress through the crack geometry and this relationship is the same for both isotropic and orthotropic plates with self-balancing loads [6]. However, many structural members have finite geometry and to account for this effect, a geometry correction factor has been incorporated into the formula relating stress intensity factor to remote stress and crack geometry. For an edge-notched tensile specimen this relationship is given as

$$K_I = F\sqrt{\pi a} \quad (3)$$

where  $a$  is crack length and  $F$  is the geometry correction factor which is a function of the ratio of crack length ( $a$ ) to width of the specimen ( $w$ ) and a formula for  $F$  is given in stress intensity factor handbooks [10] as

$$F = 1.12 - 0.231\left(\frac{a}{w}\right) + 10.55\left(\frac{a}{w}\right)^2 - 21.72\left(\frac{a}{w}\right)^3 + 30.95\left(\frac{a}{w}\right)^4 \quad (4)$$

As for correction factors, formulae such as Eq(4) developed for isotropic materials are commonly used for wood. These have been derived from either finite element method or boundary collocation methods. However, Mall et al. [9] have pointed out that these

factors for wood can be affected by directional wood properties. If stress intensity factors are derived from Eq.(1) using measured displacements, the geometry influence is automatically incorporated into the stress intensity factor and therefore, comparisons can be made between the experimentally derived factors and those established for isotropic materials.

The digital image correlation has been established as a useful tool for measuring surface displacement fields in materials. The goal of the work described in this paper is to use digital image correlation to obtain full field displacement fields near a crack tip in a plate subject to tension and use orthotropic fracture theory in conjunction with representative material properties reflecting the influence of grain angle and density to obtain stress intensity factors.

## 2. OBJECTIVES

The objectives of the research described here are to:

1. determine stress intensity factors for wood subject to tension in TL crack system using displacement fields obtained from digital image correlation in conjunction with orthotropic fracture formulae,
2. obtain geometry correction factors for  $K_I$ ,
3. establish the form of dependence of  $E_L$  on density and grain angle, and
4. attempt to establish a form of a prediction equation for fracture toughness based on density and crack angle to grain.

## 3 EXPERIMENTAL METHODS

Specimens were prepared from three 5-m long kiln-dried boards of New Zealand radiata pine (*pinus radiata*) obtained from a local sawmill in Christchurch. Specimen length x width x and thickness were 230 x 140 x 20 mm, respectively and an edge crack was cut using a fine saw blade and the crack edge was sharpened to 20mm length using a special knife prepared for the purpose. The specimen configuration is shown in Figure 1(a) and a total of 35 specimens were prepared. For each specimen, angle ( $\theta$ ) between crack plane and the RL plane was measured on the cross section. At the time of testing, average moisture content of the specimens was 15%.

Another set of 300 bending specimens of the size 300x20x20 mm were also prepared from the same material to obtain representative Young's modulus

( $E_L$ ), grain angle and density. Specimens were cut in relation to fracture specimens as shown in Figure 1(b).

### 3.1 Digital Image Correlation

Digital Image Correlation (DIC) is a non-contacting full-field strain measuring technique that has been developed to obtain full field surface displacements and their gradients (strains) of objects under stress. The DIC method has evolved over the last decade and its usefulness for measuring small displacement as occurs in engineering materials in tension and compression has been demonstrated by several investigators. For example, the method has been successfully applied to determine displacements and

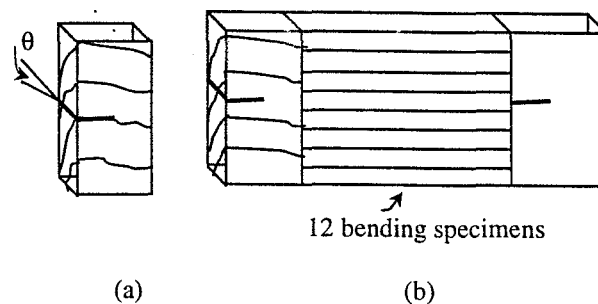


**Figure 1-** (a) Fracture specimen configuration ;  
(b) Bending specimen location with respect to a corresponding fracture specimen.

gradients of steel and aluminium with sub-pixel accuracy [11] and has recently been applied to study tension, compression and bending behavior of small wood specimens and wood joints [12,13]. Durig et al. [14] applied the method to determine stress intensity factors for aluminium in mixed-mode fracture and McNeill et al. [11] used it to obtain mode I stress intensity factors for plexiglass. It has not been used to study fracture in wood.

The theory of digital image correlation has been described in detail by several researchers but a detail treatment of the subject can be found in Sutton et al. [15]. The underlying principle of DIC is that points on the undeformed surface can be tracked to new positions on the deformed image using an appropriate error minimisation technique. To achieve this, the object surface must have a random light intensity pattern that makes a small area surrounding a point unique and able to be tracked. Therefore, specimens are usually speckled with paint or carbon toner particles to obtain a random speckle pattern on the surface. Surface is illuminated with a uniform light and the intensity distribution of light reflected by the

surface is captured by a camera and digitized and stored as a two dimensional array of grey intensity values on a computer. The experimental setup used in this study is shown in Figure 2 and a detailed discussion is given in the section on experimental method. Images captured in this study were 512x512 where each point is described by its x and y coordinates in pixels and light intensity ranging from 0 to 256 with 0 representing black and 256 white. Digitized images captured before and after deformation are then compared by a digital image correlation routine to obtain displacements and strains.

Before correlation, discrete grey intensity level array is reconstructed using bilinear interpolation to obtain a continuous intensity distribution over the whole image. To obtain displacements and gradients, a mathematical relationship between the actual displacement of a point and the light intensity of a small area surrounding the point must be established. For each small subset, displacement is defined using linear elastic theory and it is obtained by minimizing the square of the difference in light intensity between the points in the subset and all other subsets of the same size in the vicinity in the deformed image. The programme used here [16] uses cross correlation and the Newton Raphson method to perform analysis. The accuracy of the program was  $\pm 0.02$  pixels.

### 3.2 Tensile Testing and Image Capture

Tests were conducted on a computer controlled SINTECH material testing workstation. Special tensile jigs were manufactured to hold the specimen ends. The test setup with equipment used to capture images is shown in Figure 2. Specimens were speckled with black and white paint to obtain a random speckle pattern and grey level intensity histograms showed a normal distribution around the mean of 120-130. Specimens were illuminated by a fiber optic ring light level of which could be controlled. This allowed a very uniform level of illumination throughout the surface. Images were captured by an Ikigami CCD (Charge Couple Device) video camera with 25 frames per second capture rate and a lens of upto x20 magnification. Images were digitized to 512x512 size by a high accuracy 8 bit monochrome CX100 frame grabber/digitizer on an IBM 486DX66 computer. Live analogue video signal was shown on a black and white monitor and the digitized image was shown on the computer monitor.

Specimens were tested at a rate of 1 mm/min and for each specimen, 2 to 6 images were captured at various load levels upto failure. Prior to testing, a graph paper was placed against the specimen surface and its image was captured to calibrate the image distances to real

distances. A typical resolution for the current setup was 29 pixels/mm in the horizontal and 45 pixels/mm in the vertical directions, which represents a high resolution.

### 3.2 Image Processing

An area of approximately 7mm x 9mm (200x400 pixels) in front of the crack was selected for analysis. A typical subset size used to track a point was 30x30 (1mm x 0.68) and displacements for points located at

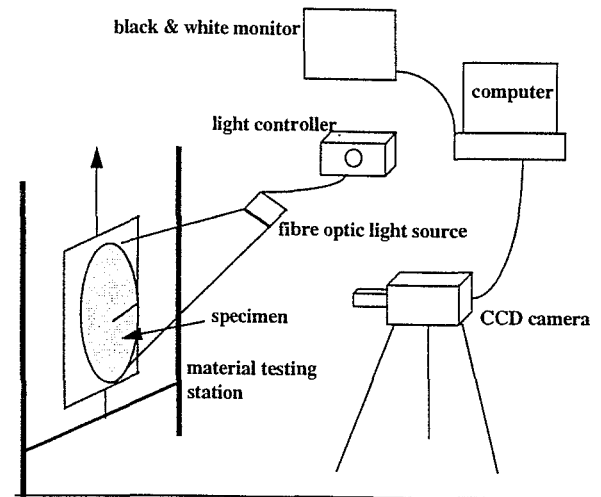


Figure 2- Schematic diagram of the test setup and image capture

15 pixel intervals which amounted to 0.5 mm horizontally and 0.33 mm vertically were obtained. Thus from one pair of images, displacements of 370 to 420 points were determined.

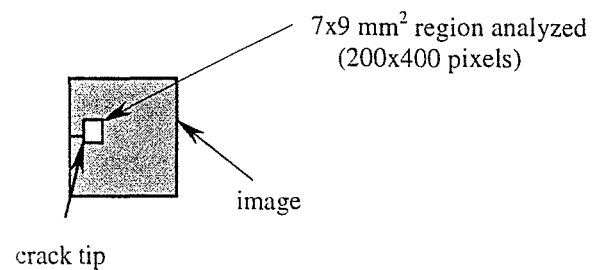


Figure 3- Location of the analysed area of the image with respect to crack tip

### 3.4 Bending Test Procedure

Prior to testing the 300 bending specimens, the grain angle was measured for each specimen as the angle ( $\theta$ ) between the tangential sawn surface and a tangent to

growth rings. Since 12 specimens were cut from each length position on the board, a broad range of  $\theta$  values varying from  $0^\circ$  and  $50^\circ$  resulted. This grain angle was equal to the angle between crack plane and RL plane measured on fracture specimens due to geometric relations. Load was applied parallel to the radial surface and three point bending tests were conducted on the SINTECH-MTS testing workstation at a rate of 1.5 mm/min. Displacement at the centre of the bottom surface was measured with respect to the neutral plane by attaching a wooden yoke carrying a high accuracy (0.001mm) dial indicator to the specimen. After testing, small samples were cut from each specimen to measure moisture content and oven-dry density. The Young's modulus was calculated using elastic beam formula for three point bending.

#### 4 COMPUTATION OF STRESS INTENSITY FACTORS

Stress intensity factors were determined by substituting experimental displacement field into theoretical field given by Eq.(1). According to fracture theory, crack tip is stationary and coincides with the origin of the co-ordinate system. The x axis lies along the crack and y axis is perpendicular to crack plane. The theoretical displacements are given with respect to the stationary crack tip. The data obtained from digital image correlation underwent a major transformation to conform to this format which required considerable time and effort in processing. As stated earlier there were approximately 375 to 426 data points within a 7mm x 9mm area in front of the tip. The Eq.(1) requires  $E_L$ ,  $E_R$ ,  $E_T$ ,  $\nu_{TL}$ ,  $\nu_{RL}$ ,  $\nu_{RT}$  and  $G_{LT}$  for the tip area. For each fracture specimen, crack angle to RL plane was known and this angle was equal to grain angle measured from bending specimens. Therefore, out of the 12 corresponding bending specimens, the one with grain angle closest to crack angle to  $R_L$  plane of the corresponding fracture specimen was selected and  $E_L$  for that specimen was used as the modulus representing the crack tip area. Other moduli were calculated in relation to  $E_L$  as in Bodig and Jayne [8] according to the relation  $E_L:E_R:E_T \approx 15:1.6:1$ , and  $E_L:G_{LT} \approx 15:1$ . Poisson ratios were obtained for Table 3.1 on page 117 of Bodig and Jayne [8] as  $\nu_{TL}=0.033$ ,  $\nu_{RL} = 0.041$ ,  $\nu_{RT}=0.47$ . The analysis was done on Mathematica [17] as follows: For a particular load level, stress intensity factor was computed by comparing the experimental displacement ( $v$ ) of all the points in the direction of applied load with that of theory using regression analysis. Specifically, the experimental  $v$  displacement was regressed against the function,  $f(r,\theta, E_i, G_{ij}, \nu_{ij})$ , given in Eq.(1) so that the stress intensity factor  $K_I$  becomes the slope of the regression line. The

procedure was repeated for other load levels and specimens.

Before proceeding to the discussion of results, a brief review of results for a typical specimen is given first. For this specimen six load levels were analysed and they were 5kN, 4.5kN, 4kN, 3.5kN, 3kN, 2.5kN. The displacement and the function value regression plot for one load level is given in Figure 4. Linear plot shows that all the experimental data points support a constant  $K$  value for a particular load level.

Table 1 shows the experimental stress intensity factors for the load levels tested along with the  $K_I$  computed from the standard formula (Eq(3)) with out correction

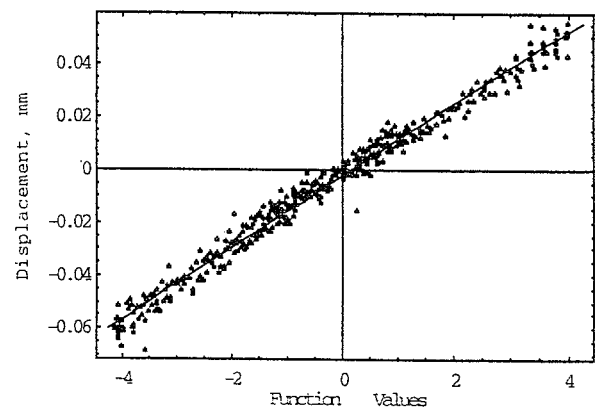


Figure 4- Regression relationship between near-tip displacement and function value in Eq.(1).

factors. It is evident that the experimental  $K_I$  is higher than that given by the standard formula for all load levels. The relationship between  $K_I$  and load level can be best described by a nonlinear relationship given in Eq.(5) with  $R^2 = 0.998$ .

$$K_I = 0.0171834 - 0.00985893P + 0.00250455P^2 \quad (5)$$

where,  $P$  is applied load in kN and  $K_I$  is in  $\text{GPa}\sqrt{\text{mm}}$ .

The fracture toughness calculated for the observed maximum load (5.7kN) for this specimen from the above Eq.(5) is 1339  $\text{kPa}\sqrt{\text{m}}$  and corresponding  $K_I$  from standard formula 501  $\text{kPa}\sqrt{\text{m}}$  as given in Table 1. From the results, correction factor ( $K_{I(\text{exp})}/K_{I(\text{standard})}$ ) was also computed and shown in Table 1 which shows that the correction factor is not a constant but varies nonlinearly with the load level. Note that for this and all other specimens,  $a/w$  is 0.143 and  $b/w = 0.821$  for

which the correction factor from the handbook formula (Eq.(4) is 1.25. What these results indicate is that for the tested specimen configuration, standard correction factor is applicable only at low load (below 3.0kN in this case) and for higher loads the effect of geometry becomes significant and at the failure the difference is as great as 2.67.

As can be seen from Table 1, stress intensity factors for six load levels applied to the same specimen have been analysed. A summary of results thus obtained for 6 specimens (based on a total of 30 analysis) is given in Table 2. Only the fracture toughness obtained from the analysis for each specimen is shown along with  $K_{Ic}$  obtained from the standard formula of Eq.(3) without correction. Correction factors required for the standard formula is obtained by taking ratio of experimental  $K_{Ic}$  to standard  $K_{Ic}$  and given in Table 2.

Results show again that the experimental fracture toughness is much higher than that predicted by the standard formula indicating that larger correction factors are required. Considering the very large correction factors obtained, this issue needs to be thoroughly investigated. At the time of writing analysis was not complete and it is hoped that a better understanding of the correction factors can be gained after its completion.

Load (kN)	$K_I$ (exp) kPa√m	$K_I$ (standard) kPa√m	F (Corr.factor)
2.5	250	220	1.13
3.0	332	264	1.26
3.5	431	308	1.4
4.0	556	352	1.58
4.5	730	396	1.84
5.0	974	440	2.21
5.7(max)	1339	501	2.67

**Table 1-** Stress intensity factors from experiments and standard formula and correction factors for a typical fracture specimen

#### 4.1 Modelling of Material Property Relationships

There were a total of 300 bending test specimens from which Young's Modulus ( $E_L$ ), density, grain angle and moisture content were measured. As shown in Figure 1(b) 12 bending test specimens corresponded to each of the fracture specimens. The goal of the modelling discussed in this section is to develop a relationship between  $E_L$  and density ( $\rho$ ) along with grain angle ( $\theta$ ). Such a model is useful in generating appropriate  $E_L$  values corresponding to any density and grain angle

that are applicable to a fracture scenario being simulated. In an attempt to develop a model,  $E_L$  distribution was first plotted. It resembled a normal distribution but there was a lot of scatter around a probable normal distribution. The density and grain angle distributions appeared totally random. Initial plotting of  $E_L$  against the two variables separately and in combination revealed that the relationship must be nonlinear and the form of the relationship  $E_L = f(\rho, \theta)$  needed to be established.

In order to determine the relationship between  $E_L$  and density- grain angle combination, we resorted to the Buckingham- $\pi$  theory which states that when the relationship sought involves several variables, these variables can be divided into primary variables that contain all the fundamental units in the problem and secondary variables whose dimensions can be expressed in terms of primary quantities. Fundamental units applicable to this problem are length, mass and time through acceleration due to gravity. For this purpose, grain angle ( $\theta$ ) was divided by  $\pi/2$  to restrict its range of spread between 0 and 1. Gibson and Ashby [18] have shown nonlinear relationships between material properties and density normalized with respect to cell wall material properties and density. They state that the cell wall axial stiffness ( $E_s$ ) is constant for wood and is around 35 GPa and cell wall density ( $\rho_s$ ) is about 1500 kg/m<sup>3</sup>. We adopted this approach to normalise  $E_L$  as  $E_L/E_s$  and density as  $\rho/\rho_s$ . It can be proved from the Buckingham- $\pi$  theorem that the normalised Young's modulus can be expressed as a function of normalised density and the normalised grain angle. After various attempts with suitable forms, it was found that the expression for  $E_L$  as a function of density and grain angle (radians) is best described by the form shown in Eq (6)

$$\frac{E_L}{E_s} = C_0 \left[ C_1 - \left( \frac{\rho}{\rho_s} \right) \left( \frac{2\theta}{\pi} \right) \right]^{C_2} \quad (6)$$

The above Eq.(6) captures the basic form of the relationship between  $E_L$  and density as well as that between  $E_L$  and grain angle. The relationship shown is a general form and can be used for any data set once the coefficients are found through nonlinear regression. These constants for the specific data set used here were found to be:  $C_0 = 0.168986$ ;  $C_1 = 0.275611$ ;  $C_2 = -0.036015$  with  $R^2 = 0.956$  for the relationship expressed.



#### 4.2 Fracture toughness and material properties

The data gathered so far support the following relationship between  $K_{IC}$  and the group of variables,  $E_L$ , density and crack angle to RL plane:

$$\frac{K_{Ic}}{E_L/E_s} = C_3 \left[ \left( \frac{\rho}{\rho_s} \right) \left( \frac{2\theta}{\pi} \right) \right]^{C_4} \quad (7)$$

In Eq.(7),  $C_3$  and  $C_4$  are constants and other parameters are the same as those defined in Eq.(6). The expression for  $E_L/E_s$  given in Eq.(6) can be substituted into Eq.(7) to obtain an expression for  $K_{IC}$  in terms of density and grain angle.

#### 5. SUMMARY AND CONCLUSIONS

Near tip displacement fields have been used in conjunction with orthotropic theory to obtain stress intensity factors for wood using representative material properties. The experimental data support a

constant stress intensity factor and follow the form depicted by theory. For a particular specimen, stress intensity factor increases nonlinearly with load, and fracture toughness for all the specimens are much greater than that obtained from standard formula indicating the need for a much larger geometry correction factor than normally used. Relationship was also established for normalised  $E_L$  as a function of normalised density and normalised grain angle based on Buckingham- $\pi$  theorem. The relationship can be useful in establishing a general relationship between  $K_{IC}$  and basic material and geometric parameters affecting fracture as briefly mentioned. Results of the complete analysis will be published in a forth coming paper.

Specimen No.	Density (Kg/m <sup>3</sup> )	$E_L$ (Gpa)	Crack angle to RL plane(deg)	Ultimate load(kN)	$K_{Ic}$ (exp) kPa√m	$K_{Ic}$ (standard Formula)	Correction Factor
1	455	7.3709	40	5.7	1339	485	2.76
2	428	5.3106	42	4.9	893	435	2.05
3	394	6.6166	23	4.5	1258	412	3.05
4	397	7.0148	19	3.0	1203	268	4.48
5	384	6.1427	15	3.5	698	306	2.28
6	422	4.8893	15	3.1	759	275	2.76

Table 2. Property data for fracture specimens and corresponding  $K_{Ic}$  and correction factors.

#### 6 REFERENCES

1. Griffith, A.A. The Phenomena of Rupture and Flow in Solids. *Philosophical Transactions, Series A*, 221, 1920, pp163-198.
2. Irwin, G.R., Analysis of stresses and strains near the end of a crack traversing a plate. *Journal of Applied Mechanics*, 24, 1957, pp361-364.
3. Irwin, G.R. Plastic zone near a crack and fracture toughness. *Sagamore Research Conference Proceedings*, 4, 1961. (as in T.L. Anderson. *Fracture Mechanics- Fundamentals and Applications*, 2<sup>nd</sup> Edition, 1994).
4. Westergaard, H.M., Bearing pressure and cracks. *Journal of Applied Mechanics*, 6, 1939, pp49-.
5. Williams, M.L., On the stress distribution at the base of a stationary crack. *Journal of Applied Mechanics*, 24, 1957, pp109-114.
6. Sih, G.C., Paris, P.C., Irwin, G.R., On cracks in rectilinearly anisotropic bodies. *International Journal of Fracture Mechanics* 1, 1965, pp189-203.
7. Triboulot, P., Jodin, P., and Pluvinaige, G. Validity of fracture mechanics concepts applied to wood by finite element calculation., *Wood Science and Technology*, 18, 1984, pp51-58
8. Bodig, J. and Jayne, B.A., *Mechanics of wood and wood composites*, Van Nostrand Reinhold Company, Inc., 1982.
9. Mall, S., Murphy, J.F., and Shottafer, J.E. Criterion for mixed-mode fracture in wood, *Journal of Engineering Mechanics*, 109, 1983, pp681-690.

- 10 Tada, H., Paris, P.C., and Irwin, G.R. *The stress analysis of cracks handbook*. 2<sup>nd</sup> Edition, Paris Productions, Inc., St. Louis, 1985.
11. McNeill, S.R.; Peters, W.H., Sutton, M.A. Estimation of stress intensity factor by digital image correlation. *Engineering Fracture Mechanics* 28(1),1987,pp101-112.
12. Zink, Audrey G; Davidson, Robert W; Hanna Robert B. Strain measurement in wood using a digital image correlation technique. *Wood and Fiber Science* 27(4), 1995,pp346-359.
13. Stelmokas, J.W., Zink, A.G., and Loferski, J.R., Image correlation analysis of multiple-bolted connections, *Wood and Fiber Science*, 29(3), 1997, pp210-227.
14. Durig, B., Zhang, F., McNeill, S.R., Chao, Y.J., and Peter, III, W.H., A study of mixed mode fracture by Photoelasticity and digital image analysis. *Optics and Laser engineering*. 14, 1991,
15. Sutton, M.A.; Wolters, W.J.; Peters, W.H.; Rawson, W.F.; McNeill, S.R. Determination of displacements using an improved digital image correlation method. *Image and Vision Computing* 1(3), 1983, pp133-139.
16. Vic-2D. Version 2.1 Digital Image Correlation, Cimpiter, Inc. USA.1998.
17. Mathematica (Version 3) Wolfram Research, 1997.
18. Gibson, L.J. and Ashby M.F., *Cellular Solids*, 2<sup>nd</sup> Edition, Cambridge University Press, London, 1997.